arXiv:1601.01609v1 [cond-mat.mes-hall] 7 Jan 2016

Experimental determination of tunneling characteristics and dwell times from temperature dependence of $Al/Al_2O_3/Al$ junctions

Edgar J. Patiño and N. G. Kelkar[1]

[1] *Departamento de Física, Universidad de los Andes, Cra.1E No.18A-10, Bogotá, Colombia*

(Dated: January 8, 2016)

Measurements of current-voltage (I-V) characteristics of a high quality $Al/Al_2O_3/Al$ junction at temperatures ranging from 3.5 K to 300 K have been used to extract the barrier properties. Fitting results using Simmons' model led to a constant value of barrier width $s\sim$20.8 Å and a continuous increase in the barrier height with decreasing temperature. The latter is used to determine the energy band gap temperature dependence and average phonon frequency $\omega = 2.05 \times 10^{13}$ sec^{-1} in Al_2O_3, which adds confidence to the precision of our measurements. The barrier parameters are used to extract the temperature dependent dwell times in tunneling ($\tau_D = 3.6 \times 10^{-16}$ sec at mid-barrier energies) and locate resonances above the barrier.

PACS numbers: 73.40.Sx,63.20.dd,03.65.Xp

Quantum tunneling has been widely used in order to investigate the density of states of the materials across the barrier[1,2] and magnetoresistance in magnetic tunnel junctions (MTJs). In most tunnel junction experiments ultra thin Al_2O_3 has been the standard choice for barrier material. In spite of the possible applications there is no clear understanding of the barrier parameters as a function of temperature. Experiments carried out previously have found an "anomalous" temperature dependence of the current voltage characteristics of Al_2O_3 tunnel junctions[3–7]. The characteristics were originally termed anomalous since the temperature dependence was found to be greater than that corresponding to the temperature change of the Fermi-Dirac distribution of electrons in the electrodes. Using Simmons model[8,9], it was found that the metal-insulator barrier height decreases with increasing temperature. The possible explanations have been controversial. This effect has been attributed to the band gap temperature dependence, the change in the dielectric space charge and trap levels in the insulator[6,7]. This last mechanism, if true, would prevent the electrons from direct tunneling[10]. On the other hand, the barrier width is a parameter which has been difficult to interpret given the fact that it need not be the same as the oxide thickness as it also depends on image forces[8,9]. There are two reports using Simmons's model on variations of the barrier width as temperature changes[6,11]. As a result of barrier shorts in MTJs[11], the apparent barrier parameters extracted from Simmons's model showed an increase of barrier width with decreasing temperature. Conversely, a small decrease of barrier width was also reported in[6,11] without any clear explanation. For ultrathin Al_2O_3 barriers other complications such as pinholes, barrier shorts and barrier regions thinner than the average barrier thickness (i.e. "hot spots") may arise in the fabrication. These may even occur in experiments where advanced plasma oxidation techniques have been used[11,12].

The present work focuses on the temperature dependence of the tunneling phenomena across Al_2O_3. We find no appreciable variation of the barrier width as a function of temperature and a mild temperature dependence of the barrier height. Furthermore, using barrier height temperature dependence we demonstrate that it is possible to directly link the barrier height and the energy gap of ultra thin Al_2O_3, assuming a simple linear relation. Thus we are able to extract important quantities, not well known, such as band gap at zero temperature, average phonon frequency and the coupling constant related to electron phonon coupling[13]. The phonon frequency when compared with the value reported in literature from sophisticated experiments corroborates the accuracy of our experimental findings. These results lead us to conclude that the main contribution to the temperature dependence of the I-V characteristics in Al_2O_3 tunnel junctions comes from the semiconductor band gap temperature dependence leaving out dielectric space charge effect and trap levels in the insulator. Finally we used the experimentally extracted barrier height and width parameters to calculate the tunneling time, which, is being reported here for a solid state tunnel junction. The order of magnitude of this time corresponds to the one obtained in sophisticated experiments involving laser induced tunneling of electrons[14].

High quality $Al/Al_2O_3/Al$ planar junctions were fabricated as a result of carefully proceeding with the following steps. Given the high Al_2O_3 resistivity, Aluminium junctions on Silicon require a very good electrical insulation from the Si layer. Therefore, a thick SiO_2 layer is needed as a base layer in order to prevent current runaway through the substrate. For this reason the Si(100) substrate was oxidized under 1100^o C in an oven for a 6 hour period. This permitted to obtain a thick SiO_2 layer of ∼300 nm. Using a HV e-gun evaporation system, each of the layers were grown in a chamber with a base pressure better than 1×10^{-7} Torr and evaporation pressure less than 1×10^{-6} Torr. The film thickness was monitored during growth to better than 1 Å by quartz balance. Thin Aluminium layers (∼30 nm) grown in this way were very uniform and did not show any pinholes as

verified by optical imaging. Our $Al/Al_2O_3/Al$ junctions were fabricated using a series of mechanical masks (inset Fig. 1b). The first step was to evaporate a 30 nm Al bottom electrode under a high deposition rate of about a 10 Å/sec. Then the sample was removed from the chamber and allowed to oxidize in air at room temperature for a period longer than 20 days. This oxidation method was preferred given its lowest oxidation rate as compared to more sophisticated methods such as oxygen plasma and dry oxygen methods. The former may lead to shorts and pinholes or "hot spots"[11,12] and the latter compared to the present work does not produce a more robust oxide layer as will be discussed later.

In order to define the junction geometry, 50 nm of SiO was evaporated in two steps through masks after oxidation totaling to 100 nm of insulation. Using a final mask, the top Al electrode (∼30 nm) was deposited. Tunnel junction areas of 375 μm × 346 μm were obtained as checked by optical microscope measurements (Inset Fig. 1b). The above fabrication process was the result of preliminary experiments on more than 20 junctions of different sizes and oxidation times leading to the final device presented here. The present results can be reproduced by carefully repeating the above steps.
Current-Voltage (I-V) characteristics were acquired in a four terminal geometry. Here a high precision dc current source provided the current while the voltage was measured using a nano-voltmeter. A large number of I-V characteristics were obtained in the temperature range between 3.5 K and 300 K. Prior to each measurement, the temperature stability was better than 1 mK. The current and voltage through the junction were kept below 1 μA and 0.7 V respectively in order to prevent overheating. Sufficient heat sinking was demonstrated in the junction as no hysteresis was observed after cycling the current two or more times at each temperature. Furthermore, performing measurements with the device on different days demonstrated high reproducibility of the I-V characteristics over time. The results are shown in Fig. 1a where only a few I-V curves are depicted out of a total of 23. To check the barrier quality, the resistance vs temperature (RT) characteristic of the tunnel junction was obtained, at 0.5 V bias voltage, indicating an insulator like temperature dependence of R (triangles Fig. 1b). More importantly a junction area resistance product $AR_N \sim 6\times10^{10}\mu m^2$ was calculated at high voltages. This value is substantially higher than those of other works using pure oxygen[2] and specialized oxidation techniques[1,15] confirming the superior quality of our junctions. The tunneling current variation as a function of temperature was also obtained at a bias voltage of 0.5 V (Fig. 1b circles). Here an increase of about 36% is observed between 3.5 and 300 K. Clear differences of the IV curves and tunneling currents demonstrate the "anomalous" temperature dependence of the current voltage characteristics. Note also that I-V characteristics are slightly asymmetrical for voltages larger than ∼0.1 V depending on the electrode's polarity. When the top electrode is positively charged (forward bias) the tunneling current is slightly lower as compared to the negatively charged polarity (back bias). This is the result of an effective barrier height which is slightly higher in the forward bias direction and lower in the reverse bias direction of the current. In order to investigate this further, the I-V data was carefully fitted using Simmons's model[8,9] for the case of a symmetric rectangular barrier and a free electron effective mass. All data analyses have been carried out using forward and backward current direction. Given that the results show only very small variations depending on current direction we focus on the forward bias experiment.

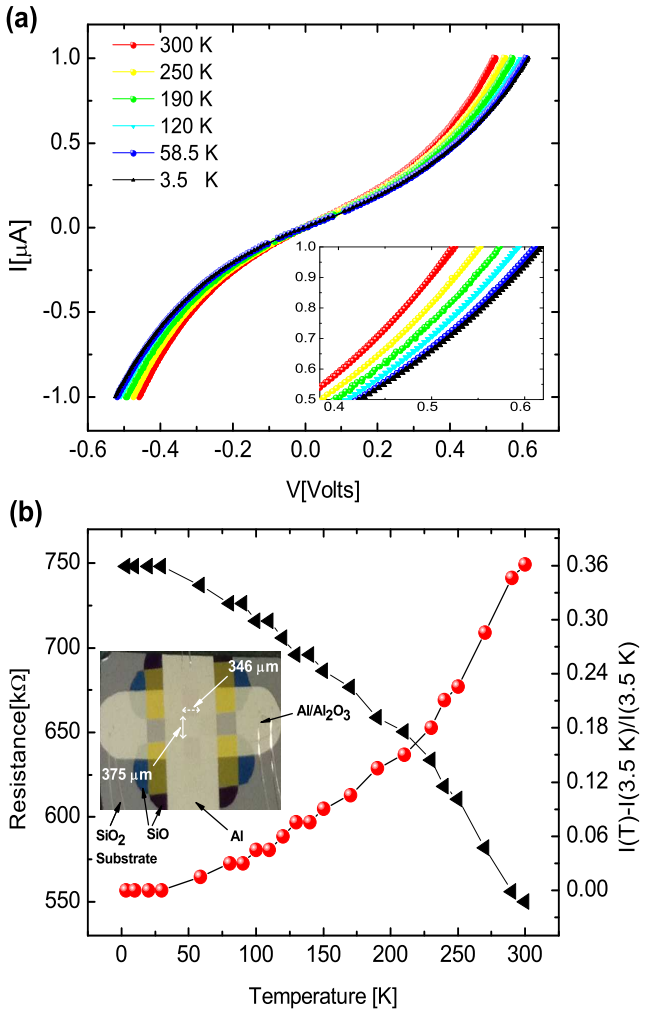

FIG. 1. (a) I-V characteristics of $Al/Al_2O_3/Al$ junctions at different temperatures; inset shows zoom in view at upper voltages. (b) Junction Resistance (triangles) and Tunneling current variation (circles) vs temperature at a bias voltage of 0.5 V; inset shows top view of $Al/Al_2O_3/Al$ junction. The junction area is defined by SiO edges between top and bottom Al electrodes.

The best fit to our data was obtained when image forces were not included. This is due to the fact that in materials with large dielectric constant K≥4 the con-

tour of a practical barrier follows closely that of a rectangular barrier[8,9]. For a dielectric material such as Al_2O_3 with K≥8 (see[16] and references therein) this is clearly the case. The junction parameters; barrier height (Φ_0), barrier width (s) and junction area (A) were determined in the intermediate voltage regime, i.e., 0≥V≤Φ_0; using the following procedure at each temperature. First a three parameter fit is performed. Remarkably, the junction area thus obtained corresponds to the value measured by the optical microscope. As explained in reference[12] this corroborates the absence of "hot spots" and pinholes in our junction. In the next step we fixed A and one of the two parameters; Φ_0 or s, while the remaining other one was extracted from an effective one parameter fit. This procedure was repeated self consistently. This led to a constant value of barrier width s∼20.8 Å with a standard error less than 0.002 at all temperatures[17]. On the other hand, Φ_0 was found to continuously decrease with temperature between the values of 1.799 eV at 300 K and 1.83 eV at 3.5 K. The barrier height thus increased as the temperature decreased from 300 to 3.5 K with a $\Delta\Phi_0 \sim 33$ meV as depicted in Fig. 2. The values found for the barrier width, height and variation are very close to the ones found in previous works (see[3,5,6] and references therein). Further analysis of our data can be obtained considering the illustration shown in inset Fig 2 where the energy gap (E_g) and barrier height (Φ_0) can be directly related in the following way. The barrier height in a tunnel junction depends on the semiconductor energy gap. Assuming a linear relation between these two parameters, we take the ratio $E_g(\mathrm{T})/\Phi_0(\mathrm{T}) = \gamma$ to be constant at all temperatures. Therefore we may calculate $\gamma = E_g(300\mathrm{K})/\Phi_0(300\mathrm{K})$ from room temperature measurements. Here Eg(300K)=3.2 eV obtained from[18] for amorphous Al_2O_3 and Φ_0(300K)=1.799 eV from our current data fit. Finally we obtain the temperature dependence of the energy gap from $E_g(\mathrm{T})=\gamma\ \Phi_0(\mathrm{T})$ in the temperature range between 3.5 and 300 K as given in Fig. 2.

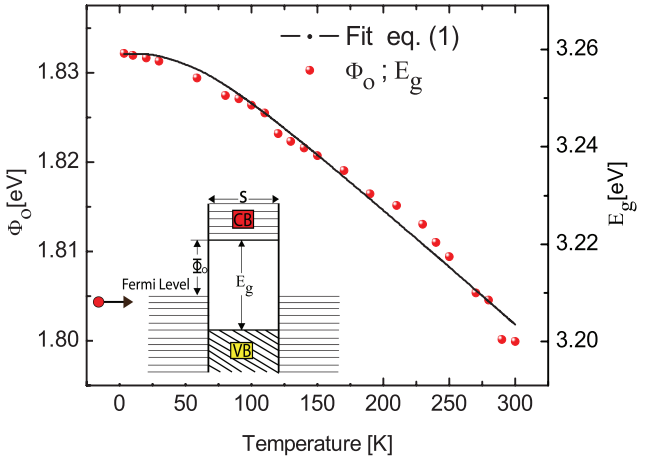

FIG. 2. Barrier height and energy gap as a function of temperature as extracted from Simmons's model and deduced from $E_g(\mathrm{T})=\gamma\ \Phi_0(\mathrm{T})$ respectively. Inset: Schematic electron energy diagram for a Metal-Semiconductor-Metal junction without voltage bias. The solid line displays the fit for the energy gap using Eq. (1).

Using the temperature dependence of the semiconductor energy gap data we can obtain additional information by fitting our experimental results to the following theoretical expression;

$$E_g(T) = E_g(0) - S\langle\hbar\omega\rangle[\coth(\langle\hbar\omega\rangle/2kT) - 1]\,, \qquad (1)$$

proposed by O'Donnel and Chen[19] as a replacement of the more commonly used Varshni equation. The authors find the formula compatible with assumptions regarding the influence of phonons on the energy band gap. $E_g(0)$ in (1) is the band gap at zero temperature, S a dimensionless coupling constant and $\langle\hbar\omega\rangle$ is the average phonon energy. We obtain an excellent fit with the values[20] $E_g(0)$=3.26 eV (standard error 0.001), S = 1.414 (standard error 0.065) and $\langle\hbar\omega\rangle$=13.5 meV (standard error 0.0016) as can be seen in Fig 2 solid line. This fit allows us to determine an average phonon frequency of $\langle\omega\rangle = 2.05\times10^{13}$ sec^{-1}. In order to compare this value with other experiments, we use the speed of sound measurements of amorphous Al_2O_3 ($v_{Al_2O_3}$) obtained using the picosecond ultrasonic technique by Rossignol et. al.[21]. Here speed of sound yields the longitudinal sound velocity $v_{Al_2O_3} = 6.7\times10^3$ m/s. Considering a lattice parameter $a \sim 4.7$ Å and a value of k=$\pi/2a$ at the middle of the first Brillouin zone, from the expression $\omega = v_{Al_2O_3}$ k; the phonon frequency $\omega = 2.24 \times 10^{13}$ sec^{-1} is obtained. Indeed these two values are exceedingly close giving us confidence on the accuracy of our measurements.

Having extracted the tunneling barrier heights from the I-V characteristics data, we now turn to the evaluation of the time spent by the electrons in the barrier region. Though the time spent by the electron interacting with the semiconductor while tunneling is expected to be tiny and not directly measurable, a knowledge of the barrier parameters obtained from data does enable us to calculate this time. We choose to calculate the so-called average dwell time of the electron in the barrier from among the several definitions available in literature. This time concept was first introduced by Smith[22] in the context of quantum collisions as the average time spent by the interacting particles in a given region of space and seems to have emerged over the years as one of the most useful concepts with a physical significance[23]. For an arbitrary barrier $V(x)$ in one-dimension, the standard dwell time for a particle with energy E is given as[24] $\tau_D(E) = [\int_{x_1}^{x_2} |\Psi(x)|^2\,dx]/j$, where x_1, x_2, are the classical turning points corresponding to $E = V(x)$. Intuitively, the time spent by the particle with velocity v can be written as $t = \int_{x_1}^{x_2} dx/v = \int \rho(x)\,dx/j(x)$, where the probability current density $j = \rho v$ with the probability density $\rho = |\Psi(x)|^2$ for $\Psi(x)$ which is a solution of the time independent Schrödinger equation. Since ρ is time independent, the continuity equation $\vec{\nabla}\cdot\vec{j} = 0$ and j

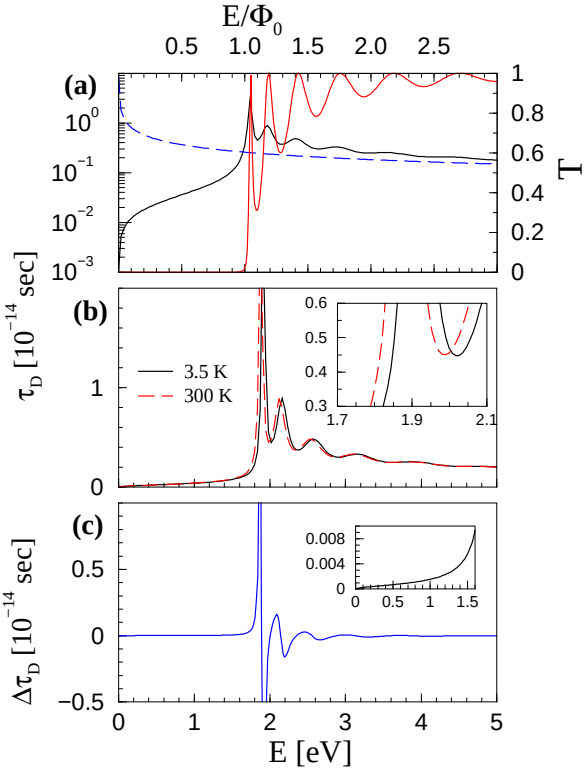

FIG. 3. Average dwell times within the potential barrier shown (a) as a function of the energy of the tunneling electrons divided by the barrier height and (b) as a function of the energy for two different temperatures. Though the difference between the dwell time curves at 3.5 and 300 K in general is negligible, in (c) we see that it becomes pronounced mostly in the resonance regions ($\Delta\tau_D = \tau_D^{300K} - \tau_D^{3.5K}$). The transmission coefficient is given by the red line with scale on the right side in (a).

($= j_x$ here) is a constant. For a plane wave e^{ikx} incident at the barrier, $j = \hbar k/m$ with $k = \sqrt{2mE}/\hbar$ and we obtain the dwell time expression given above.

For a rectangular barrier of fixed height and width, $\tau_D(E)$ can be evaluated analytically and is given for $E < \Phi_0$ as[24]:

$$\tau_D = \frac{mk}{\hbar\kappa}\frac{2\kappa s(\kappa^2 - k^2) + k_0^2 \sinh(2\kappa s)}{4k^2\kappa^2 + k_0^4 \sinh^2(\kappa s)} \qquad (2)$$

where $k_0 = \sqrt{2m\Phi_0}/\hbar$ and $\kappa = \sqrt{k_0^2 - k^2}$. For $E > \Phi_0$, one has to replace κ by iK where $K = \sqrt{2m(E-\Phi_0)}/\hbar$. Fig. 3 shows the average dwell time (which refers to the time spent in the barrier regardless of whether the particle was reflected or transmitted) as a function of the energy of the tunneling electrons at 3.5 K and 300 K. Fig 3a shows the curves as a function of the energy normalized by the barrier height (which is different at 3.5 K and 300 K) and Fig 3b shows the dwell times as a function of the energy in eV. The time shown in Fig. 3 is essentially the time spent by the electron in the $Al/Al_2O_3/Al$ sandwich in the forbidden (tunneling) region. It is 3.6×10^{-16} sec at mid-barrier energies (Fig. 3a) and hence smaller than the scale mentioned in[25] for image forces to become important. Resonances start appearing at energies above the barrier but quickly vanish around $E/\Phi_0 = 3$, where one can see that the time starts approaching the value for a free particle traversing the width of the barrier (dashed blue line in Fig. 3a). It is interesting to note that though the resonance positions in the dwell time plot are in general the same as those in the transmission coefficient (T) (red line Fig. 3a), T displays more prominently the resonances than there actually are in the dwell time curves. The average dwell time in tunneling has been shown to have the significance of a density of states[26] whereas the peaks in T simply correspond to poles (where it appears like every pole may not necessarily correspond to a sharp resonance). In Fig. 3c we plot the difference between τ_D at 300 K and 3.5 K and note that it is pronounced in the region where resonances occur.

Finally, we must mention that though all calculations in Fig. 3 are presented for the free electron mass, introducing an effective electron mass (such as 0.75 m as given in[27]) changes the barrier height and width (though only slightly) in such a way that it does not change the dwell time for electrons with $E < \Phi_0$. For energies above the barrier, the dwell time reduces for a smaller effective mass and shifts the resonances slightly. This is understandable since transmission becomes a classical effect above the barrier and lighter electrons move faster.

To summarize, we can say that the data on the I-V characteristics in an $Al/Al_2O_3/Al$ junction at different temperatures have been analysed to extract various features in the tunneling of electrons through this junction. Fitting results using Simmons's model led to a constant value of the barrier width s∼20.8 Å at all temperatures (contrary to[6]) and a continuous increase in the barrier height with decreasing temperature. The direct measurements of quantities such as the phonon frequencies and quantum tunneling times[14] require sophisticated techniques. The present work provides an indirect measurement of the same from a rather simple tunneling experiment. The average phonon frequency $\langle\omega\rangle = 2.05\times10^{13}$ sec^{-1} extracted from our tunneling experiments is exceedingly close to the one obtained from speed of sound measurements $\omega = 2.24 \times 10^{13}$ sec^{-1}. It is also remarkable that the order of magnitude of the tunneling times of the present work which ranges from 10^{-16} sec at mid barrier energies to 10^{-14} sec in the resonance region is similar to the times obtained in[14]. Similar analyses of I-V characteristics as in the present work but with other materials and multiple barriers could be useful to estimate the interaction times of electrons which are important in constructing solid state devices. With the interaction time of tunneling particles being in general a question of fundamental importance, the temperature dependent characteristics found here could have implications in other physical situations too.

We would like to acknowledge technical support from C. Talero and L. Gomez in our experimental setup and J.-

G. Ramírez for useful discussions. This work was funded by "Programa Nacional de Ciencias Básicas" COLCIENCIAS (No. 120452128168), "Convocatoria Programas 2012" Vicerrectoría de Investigaciones and "Proyecto Semilla" Facultad de Ciencias of Universidad de los Andes (Bogotá, Colombia).

[1] T. Kontos, M. Aprili, J. Lesueur, and X. Grison, Phys. Rev. Lett. **86**, 304 (2001).
[2] Kurt M. Boden, W. P. Pratt Jr and Norman O. Birge , Phys. Rev. B **84**, 020510 (2011).
[3] K. H. Gundlach and A. Wilkinson, Phys. Stat. Sol. (a) **2**, 295 (1970).
[4] O. L. Nelson and D. E. Anderson, J. Appl. Phys. 37, 77 (1966
[5] J. Kadlec, Solid-State Electronics **17**, 469 (1974).
[6] V. D. Das and M. S. Jagadeesh, Phys. Stat. Sol. (a) **66**, 327 (1981).
[7] D. Meyerhofer and S. A. Ochs, J. Appl. Phys. **34**, 2535 (1963).
[8] J. G. Simmons, J. Appl. Phys. **34**, 1793 (1963).
[9] J. G. Simmons, J. Appl. Phys. **35**, 2655 (1964).
[10] H. Bahlouli, K. A. Matveev, D. Ephron, and M. R. Beasley, Phys. Rev. B **49**, 14496 (1994).
[11] Johan J. Åkerman, J. M. Slaughter, Renu Whig Dave and Ivan K. Schuller, Appl. Phys. Lett. **79**, 3104 (2001)
[12] L. S. Dorneles, D. M. Schaefer, M. Carara and L. F. Schelp, Appl. Phys. Lett. **82**, 2832 (2003).
[13] K-C Chiu, Y-C Su and H-A Tu, Jpn. J. Appl. Phys. **37**, 6374 (1998).
[14] D. Shafir, H. Soifer, B. D. Bruner, M. Dagan, Y. Mairesse, S. Patchkovskii, M. Y. Ivanov, O. Smirnova, N. Dudovich, Nature **485**, 343 (2012); P. Eckle, A. N. Pfeiffer, C. Cirelli, A. Staudte, R. Dörner, H. G. Muller, M. Büttiker, U. Keller, Science **322**, 1525 (2008).
[15] P. SanGiorgio, S. Reymond, M. R. Beasley, J. H. Kwon, and K. Char, Phys. Rev. Lett. **100**, 237002 (2008).
[16] S. Carmona-Tellez, J. Guzman-Mendoza, M. Aguilar-Frutis, G. Alarcon-Flores, M. Garcia-Hipolito, M. A. Canseco, and C. Falcony, J. Appl. Phys. **103**, 034105 (2008).
[17] Note that the current density is proportional to Φ_0/s^2 making it more sensitive to the s parameter variations rather than Φ_0.
[18] I. Costina and R. Franchy, Appl. Phys. Lett. **78**, 4139 (2001).
[19] K. P. O'Donnell and X. Chen, Appl. Phys. Lett. **58**, 2924 (1991).
[20] Note that this values are very similar to the ones obtained for other semiconductors in[19].
[21] C. Rossignol, B. Perrin, B. Bonello, P. Djemia, P. Moch, and H. Hurdequint, Phys. Rev. B **70**, 094102 (2004).
[22] F. T. Smith, Phys. Rev. **118**, 349-356 (1960).
[23] N. G. Kelkar, H. M. Castañeda and M. Nowakowski, Eur. Phys. Lett. **85**, 20006 (2009); N. G. Kelkar, Phys. Rev. Lett. **99**, 210403 (2007).
[24] M. Büttiker, Phys. Rev. B 27, 6178 (1983).
[25] Peter J. Price, Semiconductor Science and Tech. **19**, S241 (2004); P. Scnupp, Thin Solid Films **2** 177 (1968).
[26] G. Iannaccone, Phys. Rev. B **51**, R4727 (1995); V. Gasparian and M. Pollak, Phys. Rev. B **47**, 2038 (1993).
[27] W. H. Rippard, A. C. Perrella, F. J. Albert and R. A. Buhrman, Phys. Rev. Lett., **88**, 046805, (2002).